Obour Institute Journal
for Engineering and Technology (OI-JET)
Journal homepage: https://oijet.journals.ekb.eg
Volume (2), Issue (1), December 2024

A Significant Role of Rotating Magnetic on Sn-Cu Based Lead Free Solder Alloys for Electronic Applications

Open access

Hassan M. Abd Elmoniem: High Institutes for Engineering &Technology- Obour. Km 21Cairo\ Belbies Rd.,Egypt, hassan@oi.edu.eg
Haydy Abdalla: High Institutes for Engineering &Technology- Obour. Km 21Cairo\ Belbies Rd.,Egypt
Hamada H Kora:Assistant Professor of material science and nanotechnology, Basic science Department, Bilbeis Higher Institute of Engineering, Egypt, hamada_geophy@yahoo.com

Received August 12, 2024, Revised September 5, 2024, Accepted September 15, 2024

Abstract

Due to the dangerous health effects of lead many candidates lead free solder alloys are developed for many welding applications. Sn-0.7Cu based alloys one of the most candidates for electronic applications this may be for the melting temperature and the low cost in this paper rotating magnetic field of 0.5T used with addition of (.05 co wt%) and (.5 co wt%) where the mechanical testes show strength improvement between 32-44 Mpa the tensile properties have been tested at different temperatures and different strain rate, X-ray diffraction(XRD) , optical microscope were employed to analyze the microstructure of Sn -0.7 Cu-.05 Co wt% and Sn -0.7cu -0.5Co Wt% before and after applying the rotating magnetic field(RMF), respectively and the phases were identified by energy-dispersive spectroscopy (EDS) and Differential scanning calorimetry (DSC) was used to investigate the melting temperature of which rang from 230-233 ^{0}C.

***Keywords**: Sn-Cu alloys, microstructure, electronics, rotating magnetic field.*

1. Introduction

To avoid the harmful effects of lead on the environment, lead-free solder alloys have been investigated extensively (A.A.El-Daly, et al. 2017)(Y. Liu, Y. Song, X. Li, C. Chen, K. Zhou, Ultrasonics, 2017). The formation of an unwanted denteritic phase posed a problem in terms of microstructure during solidification. The formation of columnar dendrites (EMS) was inhibited through the application of ultrasonic vibration and electromagnetic stirring in this track through solidification (A.M.El‑Taher, S.E.Abd El Azeem and A.A.Ibrahiem, 2020)(Wang X, Li T, Fautrelle Y, Dupouy MD, Jin J. 2005). During solidification, ultrasonic vibration was used initially. Ultrasonic vibration produces high intensity cavitation around the surface of the vibrator, preventing grain refining around the vibrator. Another appealing option was the application of a magnetic field during solidification. A key advantage of this technique is its contactless impact on melt flow without contamination and ease of treatment (Zeng J, Chen W and Zhang S, 2016). A high-speed rotating driver made up of an arc-like NdFeB permanent magnet and an appropriately designed arc-like NdFeB permanent magnet can form a rotating magnetic field inside metals, as demonstrated by Wang et al. (Zeng J, Chen W, Yan W, Yang Y, McLean A, 2016)(Zeng et al. (Zeng J, Chen W, Yan W, Yang Y, McLean A, 2016 ,Otsubo F, Nishida

Correspondence Author **Hassan Abd Elmoniem** hassan@oi.edu.eg

Print ISSN, 2974-4539, Online ISSN: 3062-5270

S, Era H, 2014) created an efficient F-PMS device with an acceptable magnetic field design to investigate the effects of PMS (permanent magnet stirring) on the solidification of Sn-Pb alloy at various rotational velocities (u) and centre magnetic flux densities (B). Through the use of a stirring mechanism, B. Otsubo et al. (Xinglong Sun et al 2018) studied how PMS affects grain refinement, hardness, and porosity modification in Sn-Cu-Sb alloys and Al-Cu alloys. While PMS can enhance grain refinement, it is difficult to achieve a comprehensive and satisfactory metallurgical result by using the typical PMS approach, particularly in the reduction of casting defects and improvement of segregation. As a result of these negative flaws, alloy mechanical characteristics are reduced, shrinkage porosities are increased, cavities are formed, and segregations appear, among others.In order to improve the structure and minimise solute segregation in Cu-Cr-Co-Si alloy solidification, electromagnetic fields are suggested to be used (Guang Zeng, et al 2011). The effect of a magnetic field on the microstructure, precipitate distribution, and characteristics of a Cu-Cr-Co-Si alloy was examined. Sn-Cu-X lead-free solder was examined (X: Ni, rare earths, Zn, Co, In, Ga, P, secondary particles, etc) (Meng Zhao, et al 2019). Solder junction dependability can be significantly affected by alloying elements X on melting, wettability, microstructure, interfacial reactions, and mechanical characteristics. In general, these advancements significantly improve the reliability of Sn-Cu solder connections. It is also necessary to conduct theoretical work in addition to metallurgical inquiry in order to fully understand these advances in Sn-Cu solder doping alloying elements X on multiple scales. Nagira et al. (Sansan Shuai1, et al 2019) investigated the impact of ultrasonic wave on dendritic formation of low Bi content Sn-13at %Bi alloys. The ultrasonic wave generated circulating convection with a domain size nearly equal to the small specimen size (10 X 23 mm and thickness of 300 m). It was discovered that the secondary effects of ultrasonic waves greatly aided dendritic fragmentation in the columnar zone. However, RMF-modified solidification offers a revolutionary way to improving the impact dependability of lead-free solder alloys.The influence of a rotating magnetic field (RMF) (0.5 T) on the solidification of Sn-0.7Cu-xCo (x = 0.05 and 0.5 wt%) was investigated in this study. X-ray diffraction (XRD), optical microscope (OM), scanning electron microscopy (SEM), and differential scanning calorimetry were used to explore the solidified microstructure and deformation mechanisms of Sn-Cu based lead free solder alloys at various temperatures and strain rates (DSC). The RMF process is used to create solder alloys with heterogeneous microstructures in both grain size and intermetallic compounds (IMCs).

2. Experimental details

Sn-0.7Cu based solder alloys rod doped with (0.05 wt % Co and 0.5 wt % Co) were synthesized using high purity Sn, Cu, and Co (99.99 % purity), .The melting process was carried out in quartz tube at 800 °C for one hour. The molten metals were immediately subjected to RMF during the solidification process with a natural cooling at room temperature. The details of schematic illustration of RMF can be seen in Fig. 1. Each sample's solution was remelted twice for ensuring the homogeneity, and the liquid was fluxed in a 1 cm diameter tube and allowed to cool gently at an average cooling rate of 7 ^{o}C s^{-1}. For mechanical measurements, the samples were extracted to 0.8 mm in diameter and 40 mm in length. Before testing, the specimens were annealed at 120 ^{o}C for 45 minutes to eliminate residual stress caused during sample preparation. Tensile measurements were performed at temperatures range of 25 to 110 ^{o}C using a computerized tensile testing machine. Tensile tests were also performed at constant temperatures and strain rates ranging from 10^{-5} to 10^{-3} s^{-1}. The axial strain was measured in accordance with the Active Standard ASTM E8/E8M and the Practice Standard ASTM E1012/E466 for force verification. The mechanical properties were then calculated by averaging three testing results. Temperature control

employing a thermocouple in contact with the specimen could be used to monitor the temperature of the environment chamber.

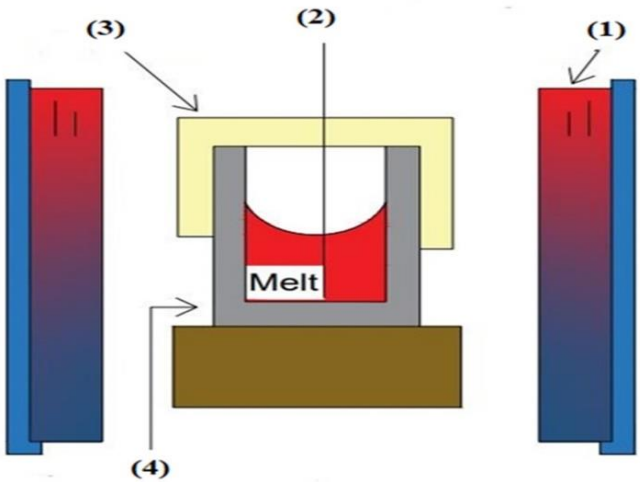

Fig. 1 Schematic diagram of the RMF experimental apparatus: 1-RMF, 2-Temperture recording system, 3-Asbestos and 4- Quartz tube.

3. Results and discussions

3.1 XRD analysis

Fig. 2 Shows the X-ray diffraction (XRD) patterns for all the prepared alloys under the effect of RMF and without the RMF. It is shown that β-Sn phase (tetragonal structure with S.G.:I41/amd) and intermetallic phases (IMC) η-Cu_6Sn_5 (Cubic structure with S.G.: Im-3m) and $(Cu,Co)_6Sn_5$ (cubic structure with S.G.: Fm-3m) can be detected with varying in the distribution of IMCs in the alloys. In Sn- 0.7Cu-0.05Co alloy (RMF=0 and RMF=0.5 T), it can obviously shown the same composition of phases can be detected are β-Sn and IMC η-Cu_6Sn_5 but IMC of $(Cu,Co)_6Sn_5$ formed by applying magnetic field. Moreover, In Sn- 0.7Cu-0.5Co, it can obviously shown the same composition of phases and IMCs are formed However, In XRD spectra, it is obvious that there is a wide peak with the maximum intensity at θ = 32.113º and observed to be slightly shifted toward smaller values of the 2θ with the applied of the magnetic fields. The peaks intensities slightly changed by applied magnetic field (A.E. Hammad, Sara El-Molla and M. Ragab, 2022).

Fig. 2, shows the integrated intensities of (220) and (211) of β-Sn phase in 0 and 0.5 T. In 0 T, the intensity of the (211) peak is higher than that of the (220) peak. By applying a rotational magnetic field (RMF) of 0.5 T, the intensity of the two peaks were (Qiang Wang, et al 2009) .enhanced, while the peaks of (420) plane are strongly dropped. It is possible to conclude that the β-Sn crystals have their c-plane parallel to the magnetic field direction. When a crystal with anisotropic magnetic susceptibility is exposed to a magnetic field, it attempts to rotate itself to an angle that minimizes system energy. One suggested explanation for the orientation of the β-Sn phases is that magnetic fields induce β-Sn crystals to rotate to a position where their c-plane is parallel to the magnetic field direction, allowing them to solidify in a lower energy state (Patterson, A. 1939).

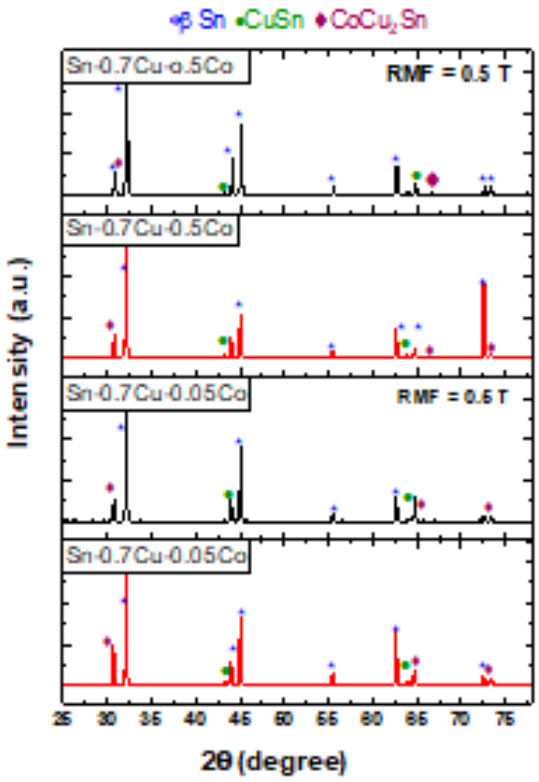

Fig. 2. XRD diffract graphs of Sn-0.7Cu-0.05Co and Sn-0.7Cu-0.5Co at RMF = 0 and 0.5 T.

3.2 .Microstructure

Fig. 3 shows the metallographic phase of the solidified alloy with and without applied field corresponding with EDX analysis for different points in each alloy. As can be seen, the solidified microstructures of both alloys are composed of the primary β-Sn phase and interdimeric IMCs: Cu_6Sn_5, and $(Cu, Co)_6Sn_5$ phases using RMF and without applied RMF during solidification. The distribution in fig.(4-a) is characterized by a large area of β-Sn grain with non-homogeneous spreading. The eutectic zones formed and were not equally distributed around the β-Sn grains. Fig. (4-c) shows that by increasing the cobalt ratio to ten times, tap worm-like IMCs were clearly generated, as shown by XRD analysis in fig. (2). The IMCs were primarily made up of $CoSn_3$, Cu_6Sn_5, and $(Cu,Co)_6Sn_5$. The presence of these phases could perform a heterogeneous nucleation site for improving the microstructure, decreasing the formation of large size spheroidal β-Sn grains, and modifying the solidification process. However, the existing magnetic field changed the size, shape, and distribution of the phases as shown in fig. 4 (b and d) (Stokes, A.R. and Wilson, A.J.C. 1944). RMF has a reasonable effect on the optimum β-Sn grain size in both solders. The β-Sn dendrites are completely re-melted and refined, as illustrated in fig. 4 (c and d), due to forced melt convection and the homogeneity of concentration and temperature fields caused by RMF. As a result of the persistent β-Sn dendritic fragmentation and increasing number of nuclei from fractured dendrites generated by the induced Lorentz force (electromagnetic force) acting on the melt, small spheroidal or equiaxed grains develop in Sn-0.7Cu-0.05Co and Sn-0.7Cu-0.5Co solders. In Fig. 4 (d), the grain size of β-Sn is reduced, but IMCs are grouped in packages with a non-homogeneous distribution, which may be attributed to the magnetic characteristics of cobalt. The results reveal that the magnetic field reduces macro segregation and fragmentation while

refining and homogenizing the existence phases. Surprisingly, the originality of the current technique will be effective for improving the thermal and creep properties of solder alloys (WuM and Liu Z-J, 2011).

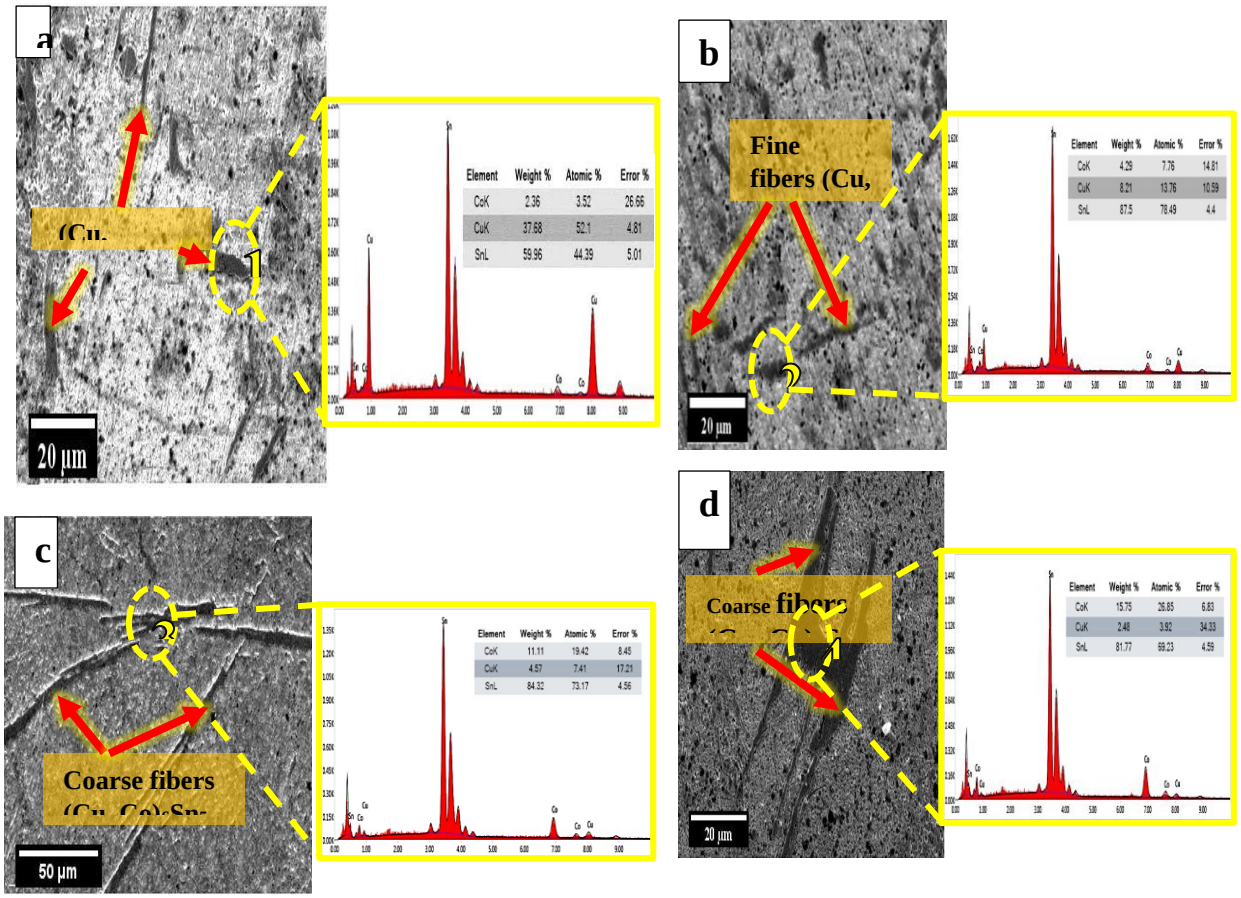

Fig. 3. High-magnifications SEM microstructure and corresponding EDS analysis of (a) Sn-0.7Cu-0.05 Co, (b) Sn-0.7Cu-.05 Co (with RMF = 0.5 T), (c) Sn-0.7Cu-.5 Co and (d) Sn-0.7Cu-.5 Co (with RMF = 0.5 T) solder alloys.

3.3 Thermal analysis

DSC analysis was used to study the effect of the rotating magnetic field on the thermal characteristics of the prepared solder alloy during heating and cooling. Fig. 4. represents the heat flow curves for the heating and cooling of the solder alloys Sn-0.7Cu-0.05Co and Sn-0.7Cu-0.5Co with applied and without applied magnetic field. The pasty range of solder alloys, as is common knowledge, is calculated using the intersection point approach as the difference between the liquidus temperature (T_{end}) and the solidus temperature (T_{onset}) during heating (T_{end}-T_{onset}). ΔT also known as undercooling of solder alloys, is the difference between the onset temperature on the heating curve and the onset temperature on the cooling curve (Xiaohua M, et al 2006). The peak temperature on the heating curve has been identified as the eutectic temperature (T_m) of the solder alloys. It is clear that Sn-0.7Cu-0.05Co and Sn-0.7Cu-0.5Co solder alloys both exhibit a single endothermic or exothermic peak. The exothermic peak of the Sn-0.7Cu-0.05Co alloy shifted from 215 ºC to 215.8 ºC because of the magnetic field application, indicating a considerable effect on solidification kinetics (Rabiger D, Eckert S and Gerbeth G, 2010). It means that the alloy quickly solidifies

in the presence of a magnetic field. The magnetic field's impact on atomic mobility or interfacial energy may be the root of the problem (Sun ZHI, Guo M, Vleugels J, et al. 2012, Jaramillo RA, Babu SS, Ludtka GM, et al. 2005, Peng YZ, Li CJ, Yang JJ, et al. 2021). The melting temperature must be considered when determining the system's maximum operating temperature. The findings are advantageous for soldering because they promote Sn nucleation, which might enhance microstructure. Lead-free solder alloys with melting temperatures below 250 °C are often favored because they don't ask for any alterations to the components, processes, or circuit boards utilized with Sn-Pb alloy. Precision range functionality is crucial for electrical applications. Porosity and hot ripping contraction during solidification are two manufacturing issues with large pasty range solders. The high values in the pasty range may also make the alloy more susceptible to vibration during welding (Yang JJ, et al. 2021). The pasty range values for the Sn-0.7Cu-0.05Co and Sn-0.7Cu-0.5Co alloys at RMF = 0T are 9.2 ^{o}C and 6.3 ^{o}C, respectively, as can be shown in Figure 5. When a magnetic field (RMF= 0.5 T) is applied, the pasty range values for Sn-0.7Cu-0.05Co and Sn-0.7Cu-0.5Co respectively fall to 3.3 ^{o}C and 5.7 ^{o}C. The pasty range values for a common eutectic lead-tin solder alloy are less than 11.0 ^{o}C. This shows that the magnetic field's application has a positive impact on undercooling. The mechanical characteristics and microstructure of solder alloys can be affected by little undercooling. The initiation of the β-Sn grains by even a small undercooling may be the cause of the refinements in IMC. The reported T values are within the specified undercooling range of Sn-Ag-Cu solder alloy, which is 10–30 ºC. This is explained by the fact that β-Sn solidification and nucleation predominantly depend on undercooling. Additionally, the Sn-0.7Cu-0.05Co solder alloy's kinetic T can be lowered by the Lorentz force of the rotational magnetic field on the melt, which can encourage the growth and nucleation of β-Sn.

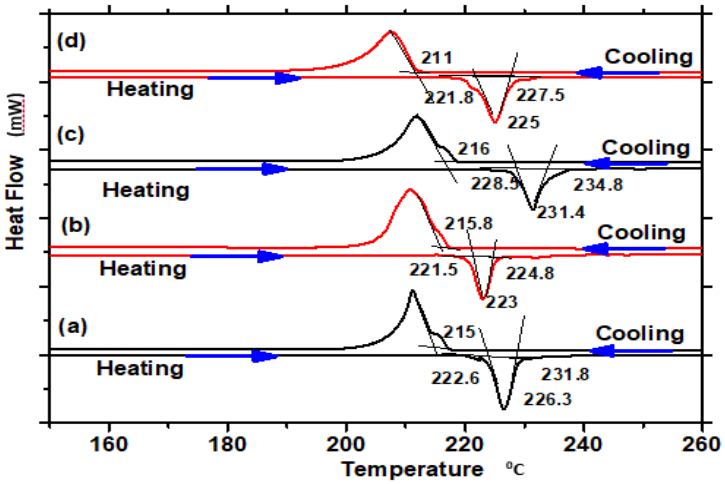

Fig. 4 (a) Sn-0.7Cu-0.05 Co ,(b) Sn-0.7Cu-0.05 Co (RMF) , (c) Sn-0.7Cu-0. 5 Co and (d) Sn-0.7Cu-0. 5 Co RMF

3.4 Mechanical properties

The solid solution strengthening of rare earth atoms, the grain refinement and stress concentration along the irregular shape of rare earth particles are considered to be the main factors affecting the mechanical properties of solder alloys.(Meng Zhao, et al.2019) microstructure observations from (SEM) and helpful of EDX and XRD in fig (2,3) showed refinement of size and distribution of β-Sn grains beside the large amount of $(Cu, Co)_6Sn_5$ .a similar investigation has been studied by A.A. El-Daly et al (A.A. El-Daly and A.A. Ibrahiem, 2018) they cleared that addition of Cu element on Sn-Bi lead free solder alloys increase yield strength (YS), the ultimate tensile

strength (UTS) and Young modulus (YM) values, while the ductility is slightly decreased. The refined microstructure and smaller dendrite β-Sn grains provide reasonable tensile of Sn-20Bi-0.5Cu alloy, owing to increasing accumulation of dislocations at grain boundaries and promotion of lattice distortion. From the results it is notable the dependence of stress and elongation on temperature the values are listed in table (1), It is evident that tensile properties (YS, UTS, and youngs modulus) for Sn-0.7Cu with .05 and .5 wt % respectively reduced by rising temperatures. That is attributed to the assumption that, with increasing temperatures, dislocations are easy to move and alloy soften easily; therefore, the tensile strength decreased. In the opposite, low temperatures lead to hardening of the alloys[26]. Obviously, the ductility is slightly increased then decreased with incompatible manners. This can be attributed to the strain rate sensitivity parameter, grain size, and variation of strain rate .(El-Taher, et al. 2023). With applying RMF (0.5 T) the values of UTS, YS and YM are increased by 20%, 21%, 18%, respectively, than the same sample without the electromagnetic field although the ductility is improved. The observed refinement of ductility and strength may be due to the rearrangement β-Sn grains with smaller area besides the refinement of IMCs where the the columnar (cu_6 Sn_5 and $cosn_3$)phases separated and repositioned through the alloy after applying RMF . in Fig(5) notably decreasing the values of stress and strain at 70 and 110 as explained before on the other wise applying the RMF on Sn-07Cu-0. 5Co the values of UTS, YS and YM are decreased by 32%, 34%, 32%, respectively, compered with Sn-07Cu-0. 5Co without magnetic field although the ductility is improved. The observed higher ductility and lower strength may be due to the dramatic decrease in the number of coarse Cu_6Sn_5 phase after applying RMF which are replaced by the lamellar eutectic structure .The high fraction of primary β-Sn phase decreases the elastic modulus and YS, which create a soft and highly compliant bulk solder.

Table 1 Mechanical property data for different solders at constant temperature 25°C and various strain rates.

Alloy	Tempreture (C °)	U.T.S (Mpa)	YS (MPa)	Elongation (%)	Youngs modulus (Gpa)
Sn-0.7Cu-0.05Co	25	43.8	41.1	49	21.9
	70	21.3	21	37.5	11
	110	20.1	19	28	10
Sn-0.7Cu-0.05Co RMF	25	56.6	54.2	52.5	28.3
	70	31.2	29.7	40.2	15.5
	110	23.4	23	24.8	11.7
Sn-0.7Cu-0. 5Co	25	30.4	28	53.5	15.2
	70	22	21	40.2	11

	110	21	20	25.5	10.5
	25	42.3	41.2	56	21.2
Sn-0.7Cu-0.5Co RMF	70	31.8	29.5	40.7	15.7
	110	28	28	27	14

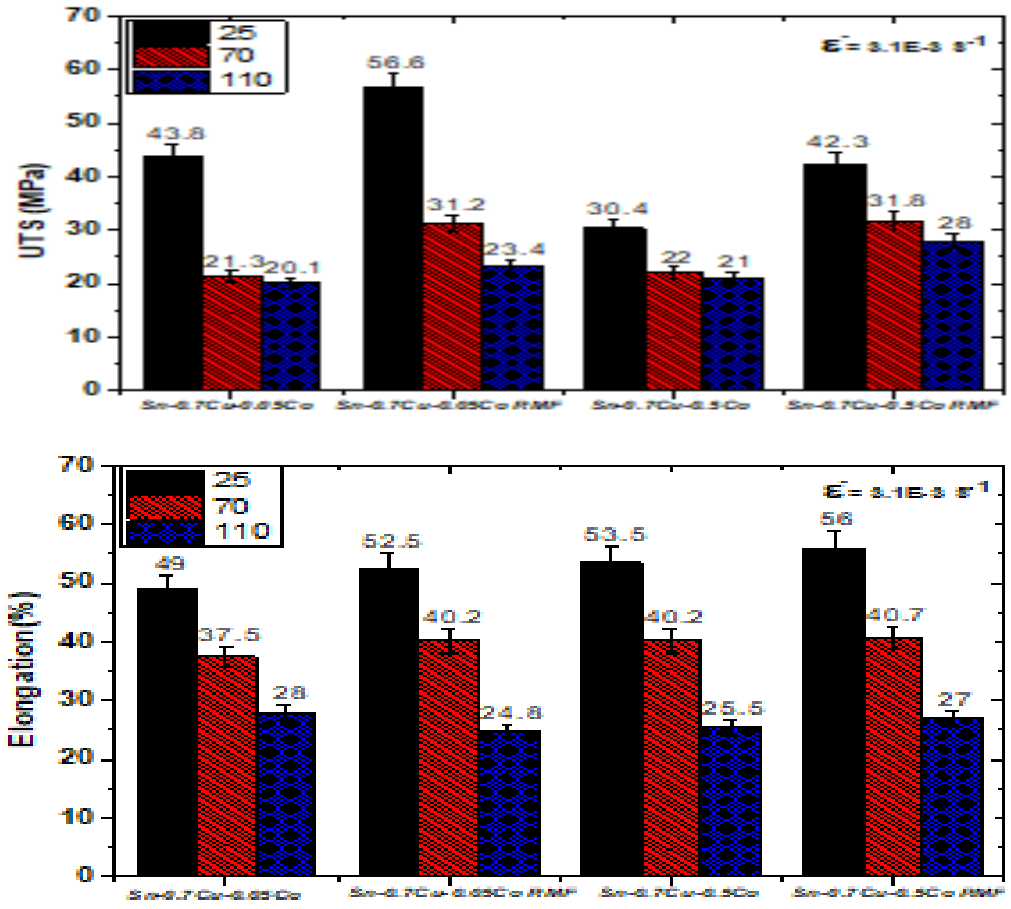

Fig. 5 comparison for Sn-0.7Cu-0.05 Co and Sn-0.7Cu-0.5 Co solder alloys with/without application of RMF at different strain rates and at different temperature

4. Conclusions

1- The minor addition of Co during solidification influences the growth and distribution of the different phases in the microstructures of the studied solder alloys.

2- The scientific results indicate a significant refining of the columnar dendrite behavior of β-Sn phase and controlling the growth of ternary phase of Sn-Cu-Co when RMF is applied on the compositions studied.

3- The RMF induced Lorentz force and magnetic moment E_m arising from the magnetic crystalline anisotropy. Equally, the thermoelectric current will be created at the liquid solid interface and at the tip of $(Cu,Co)_6Sn_5$ interface.

4- The interaction between the induced thermoelectric current and magnetic field will generate a thermoelectric magnetic force, which may induce a torque that disturbs the dendrite and rotate of the dendrite fragments ahead of the liquid solid interface.

References

1. A.A. El-Daly, A.A. Ibrahiem. Influence of rotating magnetic field on solidification microstructure and tensile properties of Sn-Bi lead-free solders, Microelectronics Reliability 81 (2018) 352–361
2. A.A. El-Daly, W.M. Desoky, A.F. Saad, N.A. Mansor, E.H. Lotfy, H.M. Abd-Elmoniem, H. B.L. Silva, A. Garcia, J.E. Spinelli, Complex eutectic growth and Bi precipitation in ternary Sn-Bi-Cu and Sn-Bi-Ag alloys, J. Alloys Compd. 691 (2017) 600–605.
3. A. M. El‑Taher , S. E. Abd El Azeem , A. A. Ibrahiem Journal of Materials Science: Materials in Electronics (2020) 31:9630–9640
4. A.E. Hammad, Sara El-Molla and M. Ragab, Impact of rotating magnetic field on the microstructure, thermal properties, and creep behavior during the solidification of Sn–2.0Ag–0.5Cu solder alloy, J Materials: Design and Applications 1–12, 2022
5. El-Taher, A.M., Abd Elmoniem, H.M. & Mosaad, S. Microstructural, thermal and mechanical properties of Co added Sn–0.7Cu lead-free solder alloy. J Mater Sci: Mater Electron 34, 590 (2023). https://doi.org/10.1007/s10854-023-09967-7
6. Guang Zeng, Songbai Xue ,Liang Zhang,Lili Gao J Mater Sci: Mater Electron (2011) 22:565–578 DOI 10.1007/s10854-011-0291-3.
7. Jaramillo RA, Babu SS, Ludtka GM, et al. Effect of magnetic field on transformations in a novel bainitic steel. Scrip Mater 2005; 52: 461–466.
8. Meng Zhao, Liang Zhang, Zhi-Quan Liu, Ming-Yue Xiong & Lei Sun (2019) Structure and properties of Sn-Cu lead-free solders in electronics packaging, Science and Technology of Advanced Materials, 20:1, 421-444, DOI: 10.1080/14686996.2019.1591168
9. Otsubo F, Nishida S, Era H. Solidification structure of Al-Cu and Sn-Cu-Sb alloys obtained by casting through induction stirring using permanent magnet. Mater Trans 2014;55:806e12.
10. Patterson, A. (1939). "The Scherrer Formula for X-Ray Particle Size Determination". Phys. Rev. 56 (10): 978–982.
11. Peng YZ, Li CJ, Yang JJ, et al. Effects of bismuth on the microstructure, properties, and interfacial reaction layers of Sn-9Zn-xBi solders. Metals (Basel) 2021; 11: 538.

12. Qiang Wang, Tie Liu, Chao Zhang, Ao Gao, Donggang Li and Jicheng He. Effects of high magnetic fields on solidified structures of Mn-90.4 wt% Sb hypoeutectic alloy. Science and Technology of Advanced Materials, 10 (2009) (5pp).
13. Rabiger D, Eckert S and Gerbeth G. Measurements of an unsteady liquid metal flow during spin-up driven by a rotating magnetic field. Exp Fluids 2010; 48: 233–244.
14. Sansan Shuai1, Xin Lin2, Yuanhao Dong1, Long Hou1, Hanlin Liao3, Jiang Wang, Zhongming Ren, Three dimensional dendritic morphology and orientation transition induced by high static magnetic field in directionally solidified Al-10wt%Zn alloy, materials science & technology, 2019.
15. Stokes, A.R. and Wilson, A.J.C. (1944) The Diffraction of X Rays by Distorted Crystal Aggregates-I, Proceedings of the Physical Society, 56, 174.
16. Sun ZHI, Guo M, Vleugels J, et al. Strong static magnetic field processing of metallic materials: a review. Current Opinion Solid State Mater Sci 2012; 16: 254–267.
17. T. Nagira, N. Nakatsuka, H. Yasuda, K. Uesugi, A. Takeuchi, Y. Suzuki, Impact of melt convection induced by ultrasonic wave on dendrite growth in Sn–Bi alloys, Mater. Lett. 150 (2015) 135–138.
18. Wang X, Li T, Fautrelle Y, Dupouy MD, Jin J. Two kinds of magnetic fields induced by one pair of rotating permanent magnets and their application in stirring and controlling molten metal flows. J Cryst Growth 2005;275:1473e9. 2004.11.178.
19. WuM and Liu Z-J. Effect of rotary magnetic field on microstructursse and microhardness of lead-free solder. Shenyang Univ Techn 2011; 33: 254–258.
20. Xiaohua M, Changle C, Zhenyu H, et al. Effect of rotating magnetic field on the solidification microstructures of Pb-Sn alloys. Sci China: Series E Techn Sci 2006; 49: 274–282.
21. Xinglong Sun et al 2018 IOP Conf. Ser.: Mater. Sci. Eng. 424 012070.
22. Y. Liu, Y. Song, X. Li, C. Chen, K. Zhou, Ultrasonics **81**, 167 (2017).
23. Zeng J, Chen W, Yan W, Yang Y, McLean A. Effect of permanent magnet stirring on solidification of Sn-Pb alloy. Mater Des 108:364e73. 2016.07.006.
24. Zeng J, Chen W, Zhang S. Experimental study of molten metal flow and numerical simulation of magnetic field during permanent magnet stirring and its application in continuous casting. Metall Res Technol 2016;113:609.